From Fig. 5 it is seen that near $v_m=3$ cm/sec energy starts being transferred to the bulk liquid as if the sphere were experiencing turbulence. Figure 4 shows that $|\Delta R|$ ceases to increase with increasing v_m above about 3 cm/sec. It may be that a certain density of turbulence exists in the superfluid and that this turbulence is responsible for determining the rate at which liquid is transferred by film flow. Difficulty in controlling or reproducing a given density of turbulence might account for some of the variations in transfer rates measured in different laboratories or in the same laboratory at different times. It is seen that the density of turbulence, or at least the transfer rates, can be reduced by obtaining the source liquid by film flow from other liquid. Then as the source or sink liquid is agitated mechanically, a minimum v_m is required to create additional turbulence in the superfluid. This increases $|\Delta R|$ as seen in Fig. 4. This increased rate of transfer of liquid through the film serves to remove some of the turbulence from the bulk and prevent $(\Delta h/\Delta t)$ from increasing as v_m^3 until $v_m=3$ cm/sec. At this point, perhaps the film cannot carry away additional turbulence and one observes that the energy imparted as turbulence in the superfluid starts to increase as v_m^3. Appropriate interactions enable this superfluid turbulence to be transformed into heat—phonons and rotons—and thus affect the distillation rate, $(\Delta h/\Delta t)$.

It may also be that a value of v_m near 3 cm/sec is associated with the onset of turbulence in the normal fluid. In accord with experiments[12] involving rotational oscillation of spheres and cylinders in He II, it was not possible to determine whether turbulence was being created in the superfluid or normal fluid.

[12] C. B. Benson and A. C. Hollis Hallett, Can. J. Phys. 34, 668 (1956).

PHYSICAL REVIEW VOLUME 138, NUMBER 5A 31 MAY 1965

Electron Slowing-Down Spectrum in Cu of Beta Rays from ^{64}Cu†

W. J. McConnell, H. H. Hubbell, Jr., R. N. Hamm, R. H. Ritchie, and R. D. Birkhoff
Health Physics Division, Oak Ridge National Laboratory, Oak Ridge, Tennessee
(Received 4 January 1965; revised manuscript received 12 February 1965)

The electron slowing-down spectrum of ^{64}Cu beta rays in an effectively infinite isotropic copper medium has been measured from 56 keV to 11 eV above the bottom of the conduction band with a spherical electrostatic electron spectrometer utilizing a Faraday cup and an electrometer as detector. The black-body cavity source was in the shape of two parallel coaxial disks of radioactive copper. Electrons emerged into the spectrometer through the opening between the disks. The flux varied from about 2.2×10^{-8} electrons cm^{-2} eV^{-1} per primary beta-ray cm^{-3} at 56 keV to 3.4×10^{-4} at the peak of the secondary-electron maximum at 15 eV above the bottom of the conduction band. A step at about 7 keV is identified as the sum of the Ni *KLL* Auger electrons caused by electron capture in ^{64}Cu, Cu *KLL* Auger electrons from the filling of *K* vacancies in copper atoms ionized by beta rays, and photoelectrons produced by K_α x-rays from both Ni and Cu. Less prominent steps at 800 and 250 eV are probably *LMM* Auger electrons and L_α photoelectrons, and the Compton edge from K_α x rays, respectively. The spectrum was compared above 35 eV with our extension of the Spencer-Attix continuous slowing-down theory and above 1.8 keV with the tabulation of the Spencer-Fano theory by McGinnies. Agreement with both theories was found everywhere within experimental uncertainties.

I. INTRODUCTION

A QUANTITATIVE understanding of the physical processes by which radiation interacts with matter requires a knowledge of the electron-flux spectrum within the material. Measurements[1,2] of the electron- and positron-flux spectra arising from beta-ray sources uniformly distributed in media have been reported between 1.70 MeV and about 30 keV and represent the only data on the electron-flux spectrum resulting from the slowing down of electrons in infinite, uniform, homogeneous, and isotropic media. These measurements are in good agreement as to spectral shape with a simplified version of the continuous slowing-down theory of Spencer and Fano.[3] However, the region below 30 keV has remained unexplored until now. A study of the electron-flux spectrum in this region would be of considerable value because of the large fluxes resulting from secondary-electron production and because these electrons generally have higher cross sections for interaction with matter than do electrons with higher energies.

The purpose of this work was to measure the electron flux over this important region and compare the results with theory. It is hoped that these and future measure-

† Research sponsored by the U. S. Atomic Energy Commission under contract with Union Carbide Corporation.

[1] R. D. Birkhoff, H. H. Hubbell, Jr., J. S. Cheka, and R. H. Ritchie, Health Phys. 1, 27 (1958).

[2] W. H. Wilkie and R. D. Birkhoff, Phys. Rev. 135, A1133 (1964).

[3] L. V. Spencer and U. Fano, Phys. Rev. 93, 1172 (1954).

ments will lead to a more quantitative understanding of the over-all radiation-damage process. In Sec. II of this paper the theoretical calculations are summarized. In Sec. III, the spectrometer and the design of the sources are described. The corrections needed in evaluating the data for comparison with theory are discussed in Sec. IV. The results are given in Sec. V and compared with theory.

II. THEORY OF ELECTRON SLOWING DOWN

A method for calculating the electron flux at any energy above a few keV due to the slowing down of primary and secondary electrons has been given by Spencer and Fano.[3] In this treatment the approximation to the primary electron-flux spectrum (in which the flux at any energy is given by the primary-electron density divided by the electron stopping power) is modified by considering the secondary electrons produced by the few violent collisions experienced by the primary electrons as an additional source and by considering the large energy losses due to bremsstrahlung as a "negative source." Flux calculations by the use of the Spencer-Fano theory have been tabulated by McGinnies in a recent National Bureau of Standards publication.[4] A simplified treatment of the theory has been given by Spencer and Attix[5] and reviewed by Birkhoff.[6] The simplified treatment assumes an absorbing material of low atomic number and initial electron energies such that bremsstrahlung may be neglected. Given these conditions, a uniform, isotropic, nonmonochromatic electron source of highest energy T_0 producing $N(T)$ electrons $\mathrm{cm}^{-3}\ \mathrm{eV}^{-1}\ \mathrm{sec}^{-1}$ with energies between T and $T+dT$ will result in an electron flux $y(T)$ defined by

$$y(T)=[S_z(T)]^{-1}\left\{\int_T^{T_0} N(T')dT' + \int_{2T}^{T_0} K_s(T',T)y(T')dT'\right\}, \quad (1)$$

where S_z is the stopping power of the absorbing medium as given by the Bethe[7] formula and

$$K_s(T',T)=\int_{T'/2}^{T'-T} k(T',\tau)d\tau, \quad (2)$$

where $k(T',\tau)$ is the Möller[8] probability per unit path for a transfer of energy τ from a primary electron of energy T'. It should be noted that both $k(T',\tau)$ and $S_z(T)$ are proportional to the effective atomic number of the medium. In the solution of these equations the effective atomic number was reduced by the number of electrons in each shell as the energy fell successively below each shell energy.

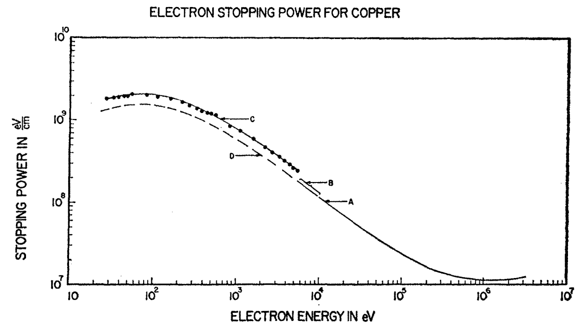

FIG. 1. Electron stopping power for copper. A. Electron stopping power taken from the supplement to Natl. Bur. Std. Circ. 577 (1958). B. Bethe-Bloch electron stopping power. C. Electron stopping power calculated from experimental proton stopping-power data assuming that protons and electrons of the same velocity slow down in the same manner. D. Curve C normalized to fit curves A and B at 5.5 keV.

Equation (1) may be solved by introducing logarithmic energy intervals to obtain a Volterra type integral equation which may be approximated by finite sums. We extended the theory to about 30 eV by using an electron stopping power obtained from experimental proton stopping power for copper[9] assuming that protons and electrons of the same velocity slow down in the same manner. The lowest proton energy at which the proton stopping power was used was 50 keV. At this energy the ratio[10] of charged to uncharged hydrogen atoms is 2:1, and this number increases rapidly as the proton energy increases. Hence the difference between electron and proton stopping power due to capture and loss of charge should be small. There still remains a 30% discrepancy between the experimental proton data and the Bethe-Bloch theory at 5-keV electron energy. If the proton data were used without adjustment, a corresponding break in the theoretical slowing-down flux would result. To avoid this misleading discontinuity, we decided to adjust the proton data to fit the electron theory at 5 keV rather than vice versa because we felt that the theory still should hold reasonably well at this energy. We feel that the uncertainty in low-energy stopping power is of the same order as other uncertainties in the slowing-down theory and data. The stopping power used is shown in Fig. 1. A more complete discussion of the theory and calculations is given elsewhere.[11]

---

[4] R. J. McGinnies, Natl. Bur. Std. (U.S.) Circ. 597 (1959).

[5] L. V. Spencer and F. H. Attix, Rad. Res. 3, 239 (1955).

[6] R. D. Birkhoff, in *Handbuch der Physik*, edited by S. Flügge (Springer-Verlag, Berlin, 1958), Vol. 34, p. 53.

[7] H. A. Bethe, in *Handbuch der Physik*, edited by H. Geiger and Karl Scheel (Julius Springer Verlag, Berlin, 1933), Vol. 24, p. 273.

[8] C. Möller, Ann. Physik 14, 531 (1932).

[9] W. Whaling, in *Handbuch der Physik*, edited by S. Flügge (Springer-Verlag, Berlin, 1958), Vol. 34, p. 202.

[10] C. F. Barnett, J. A. Ray, and J. C. Thompson, Oak Ridge National Laboratory Report No. ORNL-3113 revised, 1964 (unpublished).

[11] W. J. McConnell, H. H. Hubbell, Jr., and R. D. Birkhoff, Oak Ridge National Laboratory Report No. ORNL 3463, 1964 (unpublished).

As a check on this approximation to the theory, the slowing-down spectra in copper tabulated by McGinnies were integrated over the primary ^{64}Cu beta spectrum, and this curve is shown as a dot-dash curve in Fig. 3.

Following Spencer and Fano, we wish to normalize our experimental spectra to one primary electron born per cm^3, and have adopted their criterion that[12] "an electron emerging from a knock-on collision with energy lower than $T/2$ is classified as a secondary." However, the presence in our experimental data of extra electrons at the Auger energies presents a problem for the normalization. We shall denote as primary electrons all those which can arise from a single isolated radioactive atom, thus including nuclear beta rays + and −, internal conversion electrons, Auger electrons arising from electron capture by the nucleus, and shake-off electrons from nuclear decay. Electrons arising from violent collisions of beta particles, from photo, Compton, and pair-production effects in neighboring atoms, and all other Auger electrons such as those arising from inner-shell ionization produced by gamma rays or electrons external to the struck atom will be designated as secondaries. The "primary" Auger electrons so defined may come from the ^{64}Ni or ^{64}Zn daughters of ^{64}Cu, whereas the "secondary" Auger electrons will come almost entirely from normal ^{63}Cu or ^{65}Cu. The groups will have slightly different energies, but the resolution in this experiment is not sufficient to separate them.

The total number of primary Auger electrons of types K-XY born per disintegration in the source is given by

$$N_{KXY}=\epsilon(\epsilon_k/\epsilon)(1-\omega_k). \qquad (3)$$

Here ϵ is the number of electron captures per decay[13] 0.43; ϵ_K/ϵ is the ratio of the number of electron captures from the K shell to the total captures 0.92 as calculated from the L/K ratio[14]; and ω_K is the fluorescent x-ray yield[15] for the ^{64}Ni daughter 0.359. Strictly speaking, one should use the sum of the numbers of K vacancies created in both ^{64}Ni and ^{64}Zn daughters instead of ϵ_K. This total could be obtained by adding to ϵ the numbers of K vacancies created in each daughter by electron shake-off. However, these latter numbers are negligible for present purposes.[16] From the above numbers, N_{KXY} has the value 0.254.

The *theoretical primary* source spectrum is normalized to one primary per cm^3. Thus the sum of positive and negative beta rays and nuclear Auger electrons must be set equal to unity. Since these numbers are 0.19, 0.38, and 0.254 per decay, respectively, they then become 0.23, 0.46, and 0.31 per primary electron per cm^3. Thus the normalization equation is

$$0.31+\int_0^{T_0} N(T')dT'=1, \qquad (4)$$

where $N(T')dT'$ is the usual allowed beta energy spectrum. The integral positron and negatron spectra for ^{64}Cu are sufficiently alike in the energy range of interest here, below 50 keV, that no distinction has been made. The step of height 0.31 occurs in the primary source spectrum at approximately the Auger energy, T_K-2T_L. That is, the quantity in the braces of Eq. (1) is increased by the amount 0.31 below this energy.

The *secondary* electron part of the *theoretical* curve must be corrected by the addition of photoelectrons ejected from the K shells of nearby atoms by the x rays emitted during the K-capture process. The number as computed from Eq. (3) is 0.14 per decay or 0.17 per nuclear electron. An additional increment to the secondary-electron step comes from K vacancies created by K-shell ionization by the electrons slowing down. An integral of the theoretical flux over the K-ionization cross section as given theoretically by Arthurs and Moiseiwitsch[17] and verified experimentally by Motz and Placious[18] shows that the average electron in the flux creates 0.15 vacancies. The total height of the secondary step at energy T_K-2T_L is thus

$$0.17+0.15=0.32\frac{\text{secondary electrons cm}^{-3}}{\text{primary electron cm}^{-3}}.$$

The *experimental data* are normalized to one primary electron (+ or −) born per cm^3 by dividing the corrected experimental current by

$$D=[\rho\Lambda_0/m](0.83), \qquad (5)$$

where Λ_0 is the observed activity of the source in disintegrations per second corrected to time of removal from the reactor, ρ and m are the density and mass of the source, and (0.83) corrects disintegrations per second to nuclear electrons per second.

III. APPARATUS

The data presented here were obtained using the Keplertron, a spherical electrostatic-focusing beta spectrometer. An inverse-square electric field between two concentric charged spheres provides focusing for electrons which leave a source on the inner sphere. After energy analysis, the electrons enter a Faraday cup and are detected as a current by a vibrating-reed electrometer. Theoretically, the Keplertron as designed here has

[12] Reference 3, p. 1176.

[13] *Nuclear Data Sheets*, compiled by K. Way *et al.* (Printing and Publishing Office, National Academy of Sciences–National Research Council, Washington 25, D. C., 1962), NRC 59-2-13.

[14] M. E. Rose and J. L. Jackson, Phys. Rev. **76**, 1540 (1949).

[15] G. J. Nijgh, A. H. Wapstra, and R. Van Lieshout, *Nuclear Spectroscopy Tables* (North-Holland Publishing Company, Amsterdam, 1959), p. 81.

[16] T. A. Carlson calculates that about 0.001 K vacancies are formed per negatron or positron emission (private communication, to be published).

[17] A. M. Arthurs and B. L. Moiseiwitsch, Proc. Roy. Soc. (London) **A247**, 550 (1958).

[18] J. W. Motz and R. C. Placious, Phys. Rev. **136**, A662 (1964).

a transmission of 25%, and an energy resolution of 6.3%, while the energy of the electrons transmitted is 1.50 times the difference between inner- and outer-sphere potentials. These numbers were confirmed experimentally with the exception of the latter figure which was found to be 1.37 due to field penetration through the outer sphere. A complete description of the design, construction, and testing of the Keplertron appears in the literature.[19–21]

The cavity source consisted of two parallel coaxial copper disks 1.12 centimeters in diameter and 0.32 cm apart. Electrons emerging from the disk surface tangent to the inner sphere of the Keplertron entered the angular acceptance range of the Keplertron through the opening between the disks. Outer surfaces and edges were shielded against escape of electrons, and the two disks were joined by three thin posts 120° apart. The thickness of each disk, 0.025 centimeters, was sufficient to insure that an electron which would have been born with an energy equal to the average energy of the ^{64}Cu beta spectrum in any additional source added to the outer surface would have lost more than 90% of its energy before reaching the inner surface which emitted into the spectrometer. The source thickness thus determined was substantially thinner than the range integrated from the Bethe stopping-power formula. Thus the background from gamma radiation was reduced with a minimal decrease in absorbed energy at the inner surface. The source was hydrogen annealed for several hours at 450°C to reduce the surface oxide layer and irradiated in an inert atmosphere. The reactor irradiation produced uniformly distributed radioactivity of about 8.7 Ci in a source weighing 0.40 g. The raw data corrected only for radioactive decay are shown in Fig. 2.

Because of the extension of the flux measurements to very low electron energies, it was necessary to evaluate the response of the spectrometer, operating at low energy, to high-energy components from the source. This was accomplished in two steps. A spectrum was obtained with the open sides of the source covered with a plastic film 0.001 in. in thickness which should have cut out all electrons with energies less than 40 keV. Nonetheless, a small nearly constant current was found to persist at all spectrometer voltages, including zero, below that for 40 keV electrons, and to decay at the same rate as the source. A similar current was observed when the source was replaced by an encapsulated ^{137}Cs gamma-ray source. This current for spectrometer settings of less than 40 keV is attributed to electrons ejected by the gamma rays from the negatively biased metal surroundings of the Faraday cup and to electrons

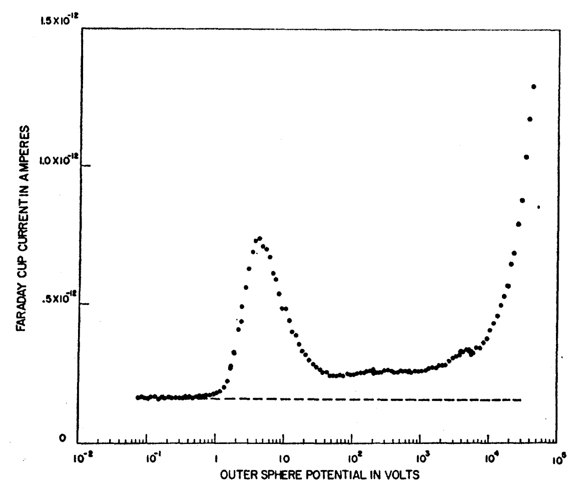

Fig. 2.

FIG. 2. Observed Keplertron current. Background current $I(0)$ due to electrons from source having more than 40-keV energy and from gamma rays is indicated by dashed line.

from the source emitted with more than 40-keV energy. These electrons are collected by the cup, which is at ground potential. The value of the current with zero volts across the spheres and no film was taken as representative of this current at higher voltages, and this value, $I(0)$ was always subtracted from observed currents as the first step in data analysis.

Although subtracting the current at zero sphere voltage from currents at higher voltages was assumed to correct data for spurious electrons of more than 40 keV, there still remained the problem of the type of correction required for spurious electrons of less than 40 keV. The latter correction was based on the observed line profiles of the spectrometer using an electron-gun analog of the radioactive source, as discussed in Ref. 21. For purposes of data correction, the over-all response was taken to be the theoretical Keplertron profile plus a continuum 0.15% of the main peak in height and extending from the main peak to 10 eV. Below this, the assumed continuum was increased to 0.3%. This composite response function, when integrated over a flux spectrum similar to that observed below 40 keV, gave a multiplicative correction to the observed flux which varied from unity at 40 keV to 0.5 at 1 eV. This response function is designated hereafter as $R(T)$.

IV. EVALUATION AND CORRECTION OF DATA

Several corrections were necessary before the observed current could be compared with the theory. The theoretical electron flux is the number of electrons per unit time integrated over all angles which would be observed crossing a spherical probe of unit cross-sectional area placed in a uniformly irradiated medium.

A correction was made for the apparent area of the source or "probe" as seen by the Keplertron. This

[19] R. H. Ritchie, J. S. Cheka, and R. D. Birkhoff, Nucl. Instr. Methods **6**, 157 (1960).
[20] R. D. Birkhoff, J. M. Kohn, H. B. Eldridge, and R. H. Ritchie, Nucl. Instr. Methods **8**, 164 (1960).
[21] H. H. Hubbell, Jr., W. J. McConnell, and R. D. Birkhoff, Nucl. Instr. Methods **31**, 18 (1964).

correction involves the geometry of the source and the angular acceptance range of the Keplertron.

For comparison with theory, the observed current $I(V)$ must be divided by the area of the source projected onto the direction of emission into the spectrometer and emitting within the angular acceptance of the spectrometer. The effective product of source area and solid angle is denoted $(A\Delta\Omega)_{\rm eff}$ and is given approximately by

$$(A\Delta\Omega)_{\rm eff}=\int_{60°}^{90°}\pi R^2\cos\theta 2\pi\sin\theta d\theta=\pi^2R^2/4 \\ =0.78\ {\rm cm}^2\ {\rm sr}, \tag{6}$$

where θ is the angle of emission from the normal to the source disk, and the angular acceptance of the spectrometer includes all electrons emitted between the tangent plane and 30-deg elevation and in all azimuths. It is here assumed that only the disk tangent to the inner sphere can emit into the spectrometer, that the shadowing effect of the upper disk can be neglected, and that the disk emits as if it were an arbitrary plane in a radioactive medium of infinite extent; i.e , that it is completely surrounded by radioactive material. The latter two assumptions are not quite correct and an attempt to estimate their importance is given in the appendix. The value of $(A\Delta\Omega)_{\rm eff}$ as calculated in the appendix and used in data correction was $(A\Delta\Omega)_{\rm eff}=0.402$ cm^2 sr.

A correction was also made for the energy barrier which the electrons must surmount as they progress from the interior of the copper metal into the vacuum. The multiplicative correction factor

$$B(T)=[1-(T_w/(T+T_w))^{1/2}]^{-1} \tag{7}$$

used was that given by Wolff,[22] and discussed by Nelson *et al.*[23] where T is the observed energy and $T_w=T_F+\varphi$ where T_F is the Fermi energy and φ is the work function. This correction ranges from 230 at $T=1$ eV to 1.1 at 1.4 keV.

The range of electron energies accepted by the spectrometer (the energy "window") is proportional to the energy, so the observed current must be divided by this window width, $T/16$, to obtain the number per unit energy.

A final correction was necessary because the Keplertron detects only negatrons. The observed negatron flux $y(T)_{\rm obs}$ is composed of components due to the primary negatrons, $y(T)_{{\rm pri},n}$; secondaries produced by primary positrons, $y(T)_{{\rm sec},p}$ and secondaries produced by primary negatrons, $y(T)_{{\rm sec},n}$ and is given by

$$y(T)_{\rm obs}=y(T)_{{\rm pri},n}+y(T)_{{\rm sec},p}+y(T)_{{\rm sec},n}. \tag{8}$$

The total flux $y(T)$ without regard to the sign of the charge includes also the contribution due to primary positrons, and is given by

$$y(T)=y(T)_{\rm obs}+y(T)_{{\rm pri},p}. \tag{9}$$

In the theoretical electron slowing down calculations, it is assumed that one electron of either sign is born per cm^3. This assumption was made possible by the near identity of the primary negatron and positron spectral shapes for ^{64}Cu which is even more pronounced in the integral form in which the spectra enter the calculations. Thus it is desirable to obtain a conversion factor by which to multiply the experimental results in order to compare them with theory, i.e., to infer from the experimental electron flux the flux which would be observed if the Keplertron could detect the primary positron flux in addition to the components of Eq. (8). This is accomplished in the following manner. In the nuclear decay of ^{64}Cu there are two negatron disintegrations for each positron disintegration. If the stopping power for negatrons given by Bethe[7] is assumed to be identical to that for positrons given by Rohrlich and Carlson[24] for the purposes of this calculation (see the discussion of this point by Birkhoff[6]), then

$$y(T)_{{\rm pri},p}=\tfrac{1}{2}y(T)_{{\rm pri},n}. \tag{10}$$

Furthermore, if the Möller[8] and Bhabha[25] cross sections for the production of secondary electrons from negatrons and positrons, respectively, are assumed to be the same, then the secondary to primary ratios will be identical also, and the value is given by

$$\frac{y(T)_{{\rm sec},n}}{y(T)_{{\rm pri},n}}=\frac{y(T)_{{\rm sec},p}}{y(T)_{{\rm pri},p}}=\frac{A(T)}{S(T)}. \tag{11}$$

Equations (8) through (11) may be solved to eliminate all fluxes except $y(T)$ and $y(T)_{\rm obs}$ with the result,

$$y(T)=y(T)_{\rm obs}\left[1+\frac{1}{2\{1+(3/2)A(T)/S(T)\}}\right] \\ =y(T)_{\rm obs}P(T). \tag{12}$$

For comparison with theory, the observed electron fluxes were multiplied by the correction factor [ ] in Eq. (12), referred to hereafter as $P(T)$ where the ratio A/S was calculated from theory as given in Eq. (1). At 37 keV the correction increased the observed electron flux by 39% and below 100 eV by less than 1%. At the higher energy the correction depends primarily upon the relative number of positrons and negatrons in the nuclear decay and not upon the theoretical ratio A/S. Although at the lower energy the dependence upon A/S is greater and the correction is less certain, the correction is much smaller.

For comparison with theory the experimental flux

[22] P. A. Wolff, Phys. Rev. **95**, 56 (1954).
[23] D. R. Nelson, R. D. Birkhoff, R. H. Ritchie, and H. H. Hubbell, Jr., Health Phys. **5**, 203 (1961).
[24] F. Rohrlich and B. C. Carlson, Phys. Rev. **93**, 38 (1954).
[25] H. J. Bhabha, Proc. Roy. Soc. (London) **A154**, 195 (1936).

was normalized to unit source activity per cubic centimeter per second. The activity determined using a gamma scintillation spectrometer and corrected to the time the source was removed from the reactor was 5.38×10^{12} electrons/sec/cm^3 referred to hereafter as D and given by Eq. (5). This number includes the nuclear Auger electrons from the Ni daughter, as described in Sec. II. The lag between the time the spectrum was obtained and the time the activity could be determined prevented the detection of short-lived contamination. However, spectrochemical analysis of the copper before irradiation in the reactor showed it to be 99.999% pure. As a result, the activity of any short-lived contamination was expected to be negligible.

The final expression, then, used for converting the observed Faraday cup current corrected for radioactive decay into the experimental flux was

$$y(T+T_w)=\frac{4\pi}{(A\Delta\Omega)_{\text{eff}}}\frac{1}{D}R(T)B(T)P(T)\left(\frac{16}{T}\right)\times\{I(T)-I(0)\} \quad (13)$$

in units of electrons cm^{-2} eV^{-1} per primary electron cm^{-3}.

V. RESULTS AND DISCUSSION

The experimental results and the Spencer-Fano and Spencer-Attix theories are shown in Fig. 3. A step function source of electrons has been introduced into the Spencer-Attix theory at 7.0 keV as described in Sec. II. This step is caused by KLL Auger electrons and K_α photoelectrons. The Auger electrons are composed[26] of 6.55 keV Ni KLL Auger electrons caused by electron capture in ^{64}Cu and 7.03 keV Cu KLL Auger electrons from the filling of K vacancies in copper atoms ionized by beta rays. The photoelectrons are produced by 7.47-keV K_α x rays from nickel and 8.04-keV K_α x rays from copper. Since the linear absorption coefficient for a 7.5-keV x ray is 568 cm^{-1} in copper, only a negligible fraction of the x rays escape from a source 0.025 cm thick. Also, since the probability for the photoelectric effect is higher for the tightly bound shells, most of the photoelectrons will be from the L shells and appear with energies of 6.55 and 7.03 keV. As a result of these processes the ratio of electrons with the KLL energies to K vacancies is approximately 1. The less prominent step at about 800 eV is probably caused by LMM Auger electrons and L_α photoelectrons in processes similar to those described above. Although the photoelectric effect is dominant in copper at the K_α energies, Compton scattering can still occur. The small step at 250 eV may be the edge of the Compton distribution caused by the K_α x rays.

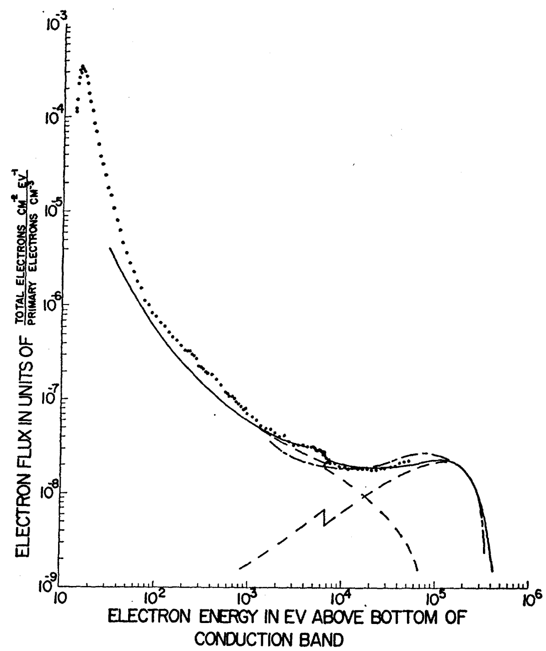

FIG. 3. Flux of electrons in copper containing uniformly distributed ^{64}Cu. Solid curve is Spencer-Attix theory and dot dash is Spencer-Fano theory. The former is broken down into primary and secondary contributions as shown by dashed lines. The step in the theoretical primary flux is calculated from experimental Auger emission data as described in Sec. II.

All in all, the absolute agreement between the experiment and the theories is excellent. In view of the fact that the theories have been extended beyond their regions of rigorous applicability and in view of the considerable uncertainties involved in attempting nuclear beta spectroscopy at these low energies, it is conceivable that the agreement is in part fortuitous.

APPENDIX

In this Appendix an estimate of the effect on the emitted current of the shadowing effect of the upper disk and posts, and of the fact that the source is not a true cavity. The correction for the latter effect is not rigorous and is only an attempt to estimate its approximate importance.

We will assume that the current emitted from the plane surface of an irradiated medium into solid angle $d\Omega$ at an angle θ from the normal is

$$I_{\text{plane}}(T,\theta)d\Omega=(1/4\pi)(1-\alpha_1)y(T)\cos\theta d\Omega, \quad (14)$$

where $y(T)$ is the flux in an infinite isotropic uniformly irradiated medium, and α_1 is the fraction of electrons which having once crossed a plane in such a medium are scattered back across it.

With the Keplertron disk source used, the observed current is that coming from the surface of the lower disk which is emitted into the solid angle between 61.4 and 90° with respect to the normal. No electrons emitted by the facing upper disk are directly observed,

[26] M. A. Listengarten, Bull. Acad. Sci. USSR Phys. Ser. **24**, 1050–1083 (1960). (English translation by Columbia Tech. Transl.) The energies used here are those of the KL_2L_3 line, which is reported to have about 61% of the total Auger intensity.

but some strike the lower disk and thus serve to improve the approximation to a cavity source. We will now calculate the approximate improvement in current effected by the presence of the second disk. The current from the upper disk which strikes area dA at r on the lower disk is obtained by integrating the current emitted by the upper disk over its surface:

$$I_2(T,r)dA=\int_{\substack{\text{area of}\\ \text{upper disk}}} I_{\text{plane}}(T,\theta)d\Omega dA', \qquad (15)$$

and one obtains

$$I_2(T,r)=\tfrac{1}{2}\{1+(R^2-H^2-r^2)/ [H^2+R^2+r^2)^2-4R^2r^2]^{1/2}\}I_{\text{plane}}(T), \qquad (16)$$

where R and H are the radii of the disks and the separation, respectively.

We now write for the total current emitted into the Keplertron acceptance angle

$$I(T)=I_1(T)+I_2(T)+I_3(T)+\cdots, \qquad (17)$$

where $I_1(T)$ is the current emitted directly by the lower disk into the acceptance angle; $I_2(T)$ is that emitted by the upper disk and reflected by the lower disk and by the shield surrounding it; $I_3(T)$ is that emitted by the lower disk and subsequently reflected by both the upper and lower disks and shields, etc. In order to evaluate the expression it is assumed that Eq. (17) can be approximated by a geometric series:

$$I(T)=I_1(T)\{1+I_2(T)/I_1(T) +[I_2(T)/I_1(T)]^2+\cdots\} \qquad (18)$$

or

$$I(T)=I_1(T)/[1-I_2(T)/I_1(T)]. \qquad (19)$$

$I_1(T)$ is given by integrating Eq. (14) over the area of the lower disk and over the solid angle in the angular acceptance range between $\theta=61.4$ and $90°$, with appropriate limits to exclude the angle subtended by the overhang of the shield around the upper disk and by the posts. We assume that a fraction α_1 of the electrons striking the lower disk and a fraction α_2 striking the lower shield are re-emitted; thus $I_2(T)$ is the sum of α_1 times the integral of $(1/\pi)I_2(T,r)\cos\theta$ over the area of the lower disk and α_2 times the integral of the same quantity over the area of the lower shield, with both integrals also being taken over the solid angle with the same limits as above and where $I_2(T,r)$ is given by Eq. (16).

One additional correction arises from the possibility that electrons from the upper disk may scatter off a large, gold-plated outer shield which surrounds only the lower disk. If a fraction α_3 of these electrons are scattered, the current from this source is given by α_3 times the integral of $(1/\pi)I_2(T,r)\cos\theta$ over the area of this shield and over the solid angle discussed above. It is assumed that a negligible number of these electrons undergo higher order scattering. The current which is observed is given by adding this correction to Eq. (19).

The final expression for the observed current may be written

$$I_{\text{obs}}(T)=Gy(T), \qquad (20)$$

where G is a numerical factor which depends on the dimensions of the source and on the values of the α's chosen. For the source which was used, $R=0.56$ cm; $H=0.32$ cm; the radius of the inner, magnesium shield was 0.75 cm; and the radius of the outer, gold-plated shield was 1.8 cm. Values of $\alpha_1=0.5$, $\alpha_2=0.4$, and $\alpha_3=0.6$ were used which were obtained from back-scattering measurements by Seliger.[27] The integrations were performed numerically on the ORNL CDC 1604 computer using Gaussian quadrature. A value for G of $0.102\,R^2$ was found. Assuming that $4\pi G$ is a better estimate for the factor $(A\Delta\Omega)_{\text{eff}}$ in Eq. (13), then $(4\pi)(0.102)R^2$ should be compared with the approximation $\pi^2R^2/4$ given by Eq. (6) We find $(A\Delta\Omega)_{\text{eff}}/4\pi G=1.92$. Thus the effective product of source area and solid angle is about half that calculated simply from Eq. (6). Previous calculations of the shadowing correction alone indicate that approximately half of this difference is due to the shadowing effect and half to the lack of a perfect cavity.

[27] H. H. Seliger, Phys. Rev. 88, 408 (1952).